

Iroquois homeobox gene 3 establishes fast conduction in the cardiac His–Purkinje network

Shan-Shan Zhang^{a,b,c,d,1}, Kyoung-Han Kim^{e,f,g,1}, Anna Rosen^{e,f,g,1}, James W. Smyth^{h,i,1}, Rui Sakuma^{c,1}, Paul Delgado-Olguin^a, Mark Davis^e, Neil C. Chi^{h,i,j,2}, Vijitha Puvindran^c, Nathalie Gaborit^a, Tatyana Sukonnik^a, John N. Wylie^a, Koroboshka Brand-Arzamendi^{h,j}, Gerrie P. Farman^e, Jieun Kim^{c,d}, Robert A. Rose^{e,f,3}, Phillip A. Marsden^g, Yonghong Zhu^c, Yu-Qing Zhou^k, Lucile Miquerol^l, R. Mark Henkelman^{k,m}, Didier Y. R. Stainier^{h,j}, Robin M. Shaw^{h,i}, Chi-chung Hui^{c,d,4}, Benoit G. Bruneau^{a,b,h,n,4}, and Peter H. Backx^{e,f,g}

^aGladstone Institute of Cardiovascular Disease, San Francisco, CA 94158; ^bProgram in Biomedical Science, ^cCardiovascular Research Institute, and Departments of ^dMedicine, ^eBiochemistry and Biophysics, and ^fPediatrics, University of California, San Francisco, CA 94143; ^gProgram in Developmental and Stem Cell Biology, Hospital for Sick Children, Toronto, ON, Canada M5G 1X8; Departments of ^hMolecular Genetics, ⁱMedicine, ^jPhysiology, and ^kMedical Biophysics and ^lDivision of Cardiology at University Health Network University of Toronto, Toronto, ON, Canada M5S 3E2; ^mMouse Imaging Centre, Toronto, ON, Canada M5G 1X8; and ⁿInstitut de Biologie du Développement de Marseille-Luminy, 13288 Marseille Cedex 9, France

Edited by Jonathan G. Seidman, Harvard Medical School, Boston, MA, and approved July 5, 2011 (received for review May 2, 2011)

Rapid electrical conduction in the His–Purkinje system tightly controls spatiotemporal activation of the ventricles. Although recent work has shed much light on the regulation of early specification and morphogenesis of the His–Purkinje system, less is known about how transcriptional regulation establishes impulse conduction properties of the constituent cells. Here we show that *Iroquois homeobox gene 3* (*Irx3*) is critical for efficient conduction in this specialized tissue by antithetically regulating two gap junction–forming connexins (Cx). Loss of *Irx3* resulted in disruption of the rapid coordinated spread of ventricular excitation, reduced levels of Cx40, and ectopic Cx43 expression in the proximal bundle branches. *Irx3* directly represses Cx43 transcription and indirectly activates Cx40 transcription. Our results reveal a critical role for *Irx3* in the precise regulation of intercellular gap junction coupling and impulse propagation in the heart.

development | electrophysiology | transcription factor

With each heartbeat, electrical impulses generated by the sinoatrial node travel through the atria, pause at the atrioventricular node, and proceed to the ventricular conduction system (VCS), also known as the His–Purkinje network. Rapid impulse conduction in the VCS tightly controls the spatiotemporal mechanical activation of the ventricles, thereby optimizing pump function (1). Conduction through the VCS is impaired in several inherited forms of cardiac conduction disorders and is associated with increased risk of arrhythmias and heart disease (2). At the cellular level, efficient impulse propagation through this network is dependent upon the interplay between cell morphology, membrane excitability, and electrical coupling of adjacent cells via gap junctions, the latter of which is the major determinant for rapid and directional conduction (3). Although regulation of early VCS specification and morphogenesis is becoming well understood (4–9), less is known about how cells of the VCS gain their specialized conduction properties as they mature.

The *Iroquois homeobox* (*Irx*) gene family of transcription factors contains a highly conserved DNA-binding homeodomain of the 3-amino acid loop extension superclass and is characterized by an 11-amino acid *Iro* motif. *Irx* genes have evolutionarily conserved roles during embryonic development (10) and can act as either repressors or activators of gene expression depending on the cellular context (11–13). All six *Irx* genes are expressed in partially overlapping patterns in the developing mouse heart (12–16). The functional significance of *Irx3* in the heart remains unknown.

Results and Discussion

We examined the developmental expression of *Irx3* in mice in which sequences encoding the *tauLacZ* fusion protein (17) were

inserted at the translational start site to create a loss-of-function reporter allele (*Irx3^{tauLacZ}*; Fig. S1A). The *tauLacZ* reporter recapitulated endogenous *Irx3* mRNA expression in the central nervous system of the developing embryo (Fig. 1A; ref. 14). At embryonic day (E) 10, a ring-like group of *Irx3^{tauLacZ+}* cells was detected in the developing ventricle. Analysis of E11 heart sections revealed that these cells represent a subset of developing trabeculae and cells surrounding the emerging interventricular septum (IVS), which are thought to contribute to the VCS (ref. 18; Fig. 1B). From E14 onwards, *Irx3^{tauLacZ}* was expressed in cells of the bifurcating His bundle primordium atop the IVS, subendocardial bundle branches along the septum, and trabeculae (ref. 18; Fig. 1C and F and Movie S1).

The adult VCS is highly asymmetric and comprises the bundle of His, subendocardial bundle branches, and Purkinje fibers (19). Cells expressing *Irx3^{tauLacZ}* matured into a highly elaborate network during postnatal maturation, marking the common His bundle, which branched into a fan-like group of smaller bundles along the left septal flank (Fig. 1G and Fig. S2A and C). In contrast, only a few thin bundles branched away from the common bundle on the right side of the heart (Fig. 1D and G, Fig. S2B, and Movie S2). These subendocardial bundles extended further toward the apex to form a dense network of interlaced fascicles connecting the free wall and septum (Fig. 1D). *Irx3* was expressed in the His bundle, which was ensheathed in a fibrous matrix in adult hearts (Fig. 1E).

At E14.5, *Irx3^{tauLacZ+}* cells were surrounded by endocardial cells marked by platelet/endothelial cell adhesion molecule-1 (PECAM) and expressed the muscle-specific actin-binding protein tropomyosin (Fig. S2D and E). These subendocardial *Irx3⁺* myocytes coexpressed established markers of the conduction sys-

Author contributions: S.-S.Z., K.-H.K., A.R., J.W.S., R.S., N.C.C., R.M.S., C.-c.H., B.G.B., and P.H.B. designed research; S.-S.Z., K.-H.K., A.R., J.W.S., R.S., P.D.-O., M.D., N.C.C., V.P., N.G., T.S., J.N.W., K.B.-A., G.P.F., J.K., R.A.R., Y.Z., and Y.-Q.Z. performed research; P.A.M. and L.M. contributed new reagents/analytic tools; S.-S.Z., K.-H.K., A.R., J.W.S., P.D.-O., N.C.C., N.G., R.A.R., Y.-Q.Z., R.M.H., D.Y.R.S., R.M.S., C.-c.H., B.G.B., and P.H.B. analyzed data; and S.-S.Z., K.-H.K., A.R., J.W.S., C.-c.H., B.G.B., and P.H.B. wrote the paper.

The authors declare no conflict of interest.

This article is a PNAS Direct Submission.

Freely available online through the PNAS open access option.

¹S.-S.Z., K.-H.K., A.R., J.W.S., and R.S. contributed equally to this work.

²Present address: University of California at San Diego, La Jolla, CA 92093.

³Present address: Department of Physiology and Biophysics, Faculty of Medicine, Dalhousie University, Halifax, NS, Canada B3H 4R2.

⁴To whom correspondence may be addressed. E-mail: bbruneau@gladstone.ucsf.edu or cchui@sickkids.ca.

This article contains supporting information online at www.pnas.org/lookup/suppl/doi:10.1073/pnas.1106911108/-DCSupplemental.

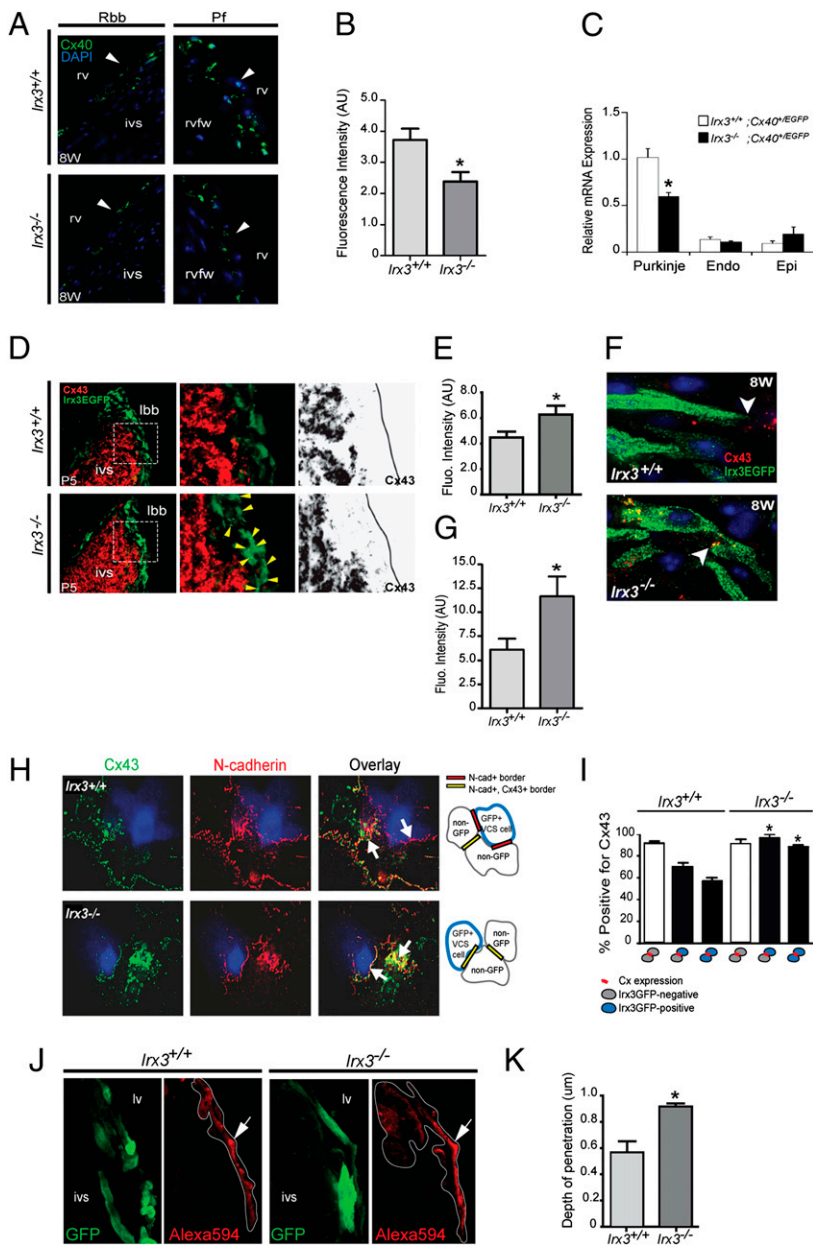


Fig. 3. *Irx3* regulates Cx40 and Cx43 expression in the VCS. (A) Representative Cx40 immunofluorescence images of the right bundle branch and right ventricular free wall Purkinje fibers of wild-type (WT) and *Irx3*-null mice at 8 wk. (B) Quantitation of Cx40⁺ plaques. (C) qRT-PCR analysis of LCM captured adult VCS cells for *Gja5* mRNA in *Irx3^{tauLacZ/tauLacZ};Cx40^{EGFP/+}* vs. *Irx3^{+/+};Cx40^{EGFP/+}* hearts. (D) Representative Cx43 immunofluorescence images. Arrowheads show ectopic Cx43⁺ plaques in *Irx3::EGFP*⁺ proximal bundle branch cells of *Irx3*-null mice at P5. Grayscale images show intensity mask for Cx43 signal. (E) Plaque intensity was quantified by using ImageJ software. **P* < 0.05 vs. WT. (F) Adult heart confocal imaging at 100× magnification shows ectopic Cx43⁺ plaques at conduction-working myocyte and conduction-conduction myocyte borders in the absence of *Irx3*. (G) Plaque intensity was quantified by using ImageJ software. **P* < 0.05 vs. WT. (H) Immunofluorescence for Cx43 (green), N-cadherin (red), and EGFP (blue) of cells reagggregated from the VCS of either WT or *Irx3*-null mice, each expressing the *Irx3::EGFP* reporter. (I) Quantitation of Cx43 plaque expression at cell-cell borders. (*J* and *K*) Fluorescent dye spread (white outline) in microinjected proximal right bundle branch cells (marked by *Irx3::EGFP*⁺). **P* < 0.05 vs. WT. *Iv*, right ventricular free wall; *Pf*, Purkinje fibers; *LBB*, left bundle branch; *Endo*, endocardium; *Epi*, epicardium.

Irx3, a higher number of cell borders between VCS cells (marked by *Irx3::EGFP*) and non-GFP⁺ working myocytes contained Cx43⁺ plaques compared with wild type (Fig. 3 *H* and *I*). The presence of Cx43 in the VCS may cause slowing of impulses through the formation of heterotypic Cx40–Cx43 gap junctions that cannot conduct impulses efficiently (32) or may be due to ectopic gap junctions coupling the VCS to the working myocardium, resulting in lateral spread of excitation.

To better understand how the observed changes in Cx expression could underlie conduction slowing, we used a dye-coupling assay (33) in which the spread of Alexa 594 from microinjected cells of the proximal right bundle branches was measured to examine intercellular communication. Dye spread was predominantly restricted within *Irx3::EGFP*⁺ VCS cells in wild-type hearts, whereas hearts lacking *Irx3* displayed significantly higher depth of dye spread from bundle branch cells to the non-GFP working myocardium (Fig. 3 *J* and *K*). These data, combined with our immunofluorescence results, demonstrate that ectopic Cx43 in the proximal conducting system allows abnormal communica-

tion between VCS cells and the working myocardium. Presumably, Cx43 expression in the myocytes of the proximal VCS allows functional gap junctions to form with the working myocardium via Cx43–Cx43 hemichannels (34–36). This abnormal coupling is expected to cause impulse dispersion away from the conduction axis, as well as to promote conduction block through charge dissipation from the smaller VCS source to the large ventricular sink.

To gain mechanistic insight into the molecular basis for the antithetic regulation of Cx40 and Cx43 by *Irx3*, we examined Cx40 (*Gja5*) and Cx43 (*Gja1*) expression in isolated neonatal ventricular myocytes (NVMs) infected with adenovirus encoding GFP, *Irx3*, dominant *Irx3* activator (*VPI6-Irx3*), or dominant *Irx3* repressor (*EnR-Irx3*; Fig. 4*A*). Infected NVMs overexpressed comparable levels of *Irx3* mRNA and protein (Fig. *S6 A* and *B*). Consistent with the observed Cx40 decrease in the VCS of *Irx3*-null mice, Cx40 protein and mRNA were increased by *Irx3* overexpression in NVMs (Fig. 4 *B* and *C*). Interestingly, *EnR-Irx3* overexpression promoted *Gja5* expression, whereas *VPI6-*

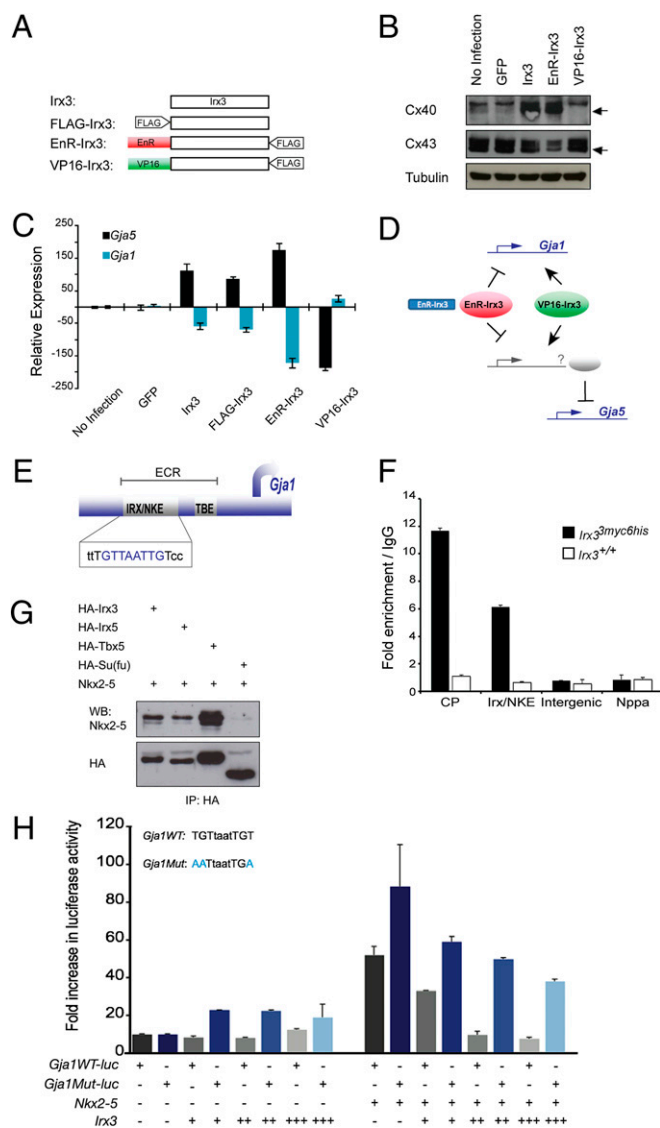


Fig. 4. Transcriptional regulation of *Cx40* and *Cx43* gene expression by *Irx3*. (A) NVMs were infected with the following adenoviral constructs: GFP control (*Ad-GFP*), *Irx3* (*Ad-Irx3*, *Ad-FLAG-Irx3*), *Irx3* fused to the VP16 activation domain (*Ad-VP16-Irx3*), or the Engrailed suppressor domain (*Ad-EnR-Irx3*). (B) *Cx40* and *Cx43* protein expression. (C) Quantitation of *Gja1* and *Gja5* mRNA compared with noninfected and GFP-infected cells. (D) Schematic depicting regulation of *Gja1* and *Gja5* transcription by dominant active and dominant negative forms of *Irx3* in infected NVMs. (E) Genome alignment analysis of the *Gja1* promoter revealed an evolutionarily conserved element containing a putative *Irx3* binding site that overlaps with an Nkx2-5 binding motif (*Irx/NKE*), immediately upstream of T-box binding elements (TBE). (F) Chromatin immunoprecipitation using ventricles from *Irx3*^{3myc-6his} mice shows enrichment of *Irx3* at the conserved *Irx/NKE* site and core promoter, but not at an intergenic region or the *Nppa* promoter. (G) Coimmunoprecipitation of *Irx3* with Nkx2-5 and Tbx5. Su(fu) serves as negative control. (H) Luciferase activity of *Gja1-luciferase* in cells cotransfected with *Irx3* or Nkx2-5 expression constructs. *Gja1mut* indicates a *Gja1-luciferase* reporter in which three point mutations were made in the evolutionarily conserved core binding sequence. ECR, evolutionarily conserved region; CP, core promoter; *Irx/NKE*, evolutionarily conserved binding site for *Irx3* and Nkx2-5.

Irx3 inhibited *Gja5* expression. This result suggests that *Irx3* likely regulates *Gja5* indirectly, activating *Gja5* expression by suppressing the transcription of a *Gja5* repressor. In contrast, our results indicate that *Irx3* directly represses *Gja1* transcription. In agreement with a repressive role of *Irx3* on *Cx43* ex-

pression in vivo, *Cx43* protein and mRNA (Fig. 4 *B* and *C* and Fig. S6 *C* and *D*) were reduced in cells overexpressing *Irx3*. Furthermore, *Gja1* mRNA was markedly decreased in the presence of *EnR-Irx3* but increased slightly in response to *VP16-Irx3*. The effects of dominant repressor and activator forms of *Irx3* on the Cx promoters is summarized in Fig. 4*D*. Given that *Iroquois* proteins commonly act as transcriptional repressors, our data support antithetical regulation of *Cx40* and *Cx43* expression by *Irx3* through direct as well as indirect mechanisms.

Promoter analysis of Cxs that are expressed in the VCS (*Cx40*, *Cx43*, *Cx45*, and *Cx30.2*) revealed that the *Gja1* promoter contains an evolutionarily conserved element harboring a putative *Irx3* binding site (37–39), which overlaps with an Nkx2-5 binding motif (*Irx/NKE*) immediately upstream of conserved T-box binding elements (Fig. 4*E*). The conserved element is 198 bp in size and is located at genomic coordinates (mm9) chr10:56,096,566–56,096,763. To determine whether *Irx3* binds the *Gja1* promoter in vivo, we performed chromatin immunoprecipitation with ventricles isolated from the *Irx3*^{3myc-6his} knock-in mouse line, which express C-terminally tagged *Irx3* protein under endogenous gene expression control (Fig. S1 *B* and *C*). Enrichment for *Irx3*^{3myc-6his} was detected at the *Gja1* promoter region containing the *Irx/NKE* element and the core *Gja1* promoter, but not at an intergenic region or at the *Nppa* promoter (Fig. 4*F*). Moreover, coimmunoprecipitation shows that *Irx3* can form a protein complex with Nkx2-5 (Fig. 4*G*). We then examined whether *Irx3* and Nkx2-5 could regulate *Gja1* transcription in vitro and found that *Irx3* indeed antagonizes Nkx2-5-dependent activation of a *Gja1-luciferase* reporter containing 1.68 kb of the endogenous promoter sequence (40) in transfected COS7 cells (Fig. 4*H*). Furthermore, three point mutations, made to alter predicted core binding sequences recognized by *Irx3*, diminished the ability of *Irx3* to exert repression of *Gja1-luciferase* in the presence of increasing amounts of Nkx2-5. In the proximal VCS, where these transcription factors are expressed at high levels, *Irx3* could therefore repress Nkx2-5-mediated activation of *Gja1* transcription. Furthermore, direct binding of *Irx3* to the *Gja1* promoter may lead to transcriptional repression through its interactions with Nkx2-5 or Tbx5 and/or through recruitment of corepressors through a mechanism similar to that of *Irx5* (13).

In this study, we demonstrate that *Irx3* is a unique transcriptional regulator of rapid electrical conduction that is necessary to drive ventricular activation. To address whether *Irx3* function is evolutionarily conserved, we examined its role in zebrafish, where the *ziro3a* ortholog is expressed in the heart at 48 h after fertilization (Fig. S7 *A* and *B*). Optical mapping was performed in live zebrafish expressing the in vivo calcium transient reporter *Tg(cmlc2:gCaMP)*^{s878} (41). Similar to our observations in mice, inhibition of *ziro3a* by morpholino antisense oligonucleotides caused slowed and abnormal impulse conduction in the ventricle (Fig. S7*C*).

Concluding Remarks

The *Irx* gene family of transcription factors has evolutionarily conserved roles during embryonic development (10) and is expressed in the developing mouse heart. We have shown that *Irx5* represses transcription of the voltage-gated potassium channel gene *Kv4.2* to establish an epicardial-to-endocardial repolarization gradient (12–16). Our present study identifies a previously undescribed role for an additional *Iroquois* factor, *Irx3*, in the tight regulation of gap junction gene expression in specialized His-Purkinje system cells, where its expression is highly enriched. *Irx3* regulation of Cx expression is likely to be relevant to the electrical maturation of other excitable cell types, such as those of the central nervous system enriched in *Irx3* expression (14, 42).

Our studies reveal an important role of *Irx3* in the precise transcriptional control of intercellular coupling and synchronized ventricular depolarization. Interestingly, the electrical phenotypes in mice lacking *Irx3* are commonly associated with inherited

increased risk of arrhythmias and heart failure (2). Furthermore, it has been shown that defects in cardiac impulse conduction can directly lead to aberrant cardiac remodeling and reduced cardiac function (43). Thus, it may be informative to determine whether deleterious mutations reside in the human *IRX3* gene.

Materials and Methods

Details of materials and methods are provided in *SI Materials and Methods*. All animal work was conducted according to the regulations provided by the Animal Care and Use Committees. β -Galactosidase and Masson's trichrome staining of fixed embryos and tissue (4% paraformaldehyde) was carried out by using standard methods. Optical projection tomography (OPT) imaging of hearts was performed as described (44). Fluorescence in situ hybridization in zebrafish was performed as described (41). For immunofluorescence detection, four-chambered view serial cryosections (8 μ m) were stained with various antisera as described in *SI Materials and Methods*. Transthoracic echocardiography was used for noninvasive serial assessment of cardiac function in mice as described (13, 45). Surface ECG (leads I and II) was obtained at P12 and at 8–10 wk as described (13). For Cx protein imaging, the Scan Large Image function of NIS Elements was used to stitch high-resolution (60 \times 1.49 Apo TIRF objective) widefield epifluorescence images encompassing the entire septum. Differences between groups were examined for

statistical significance by using the Student *t* test. $P < 0.05$ was regarded as significant.

ACKNOWLEDGMENTS. We thank V. Vedantham for initial help with FACS; B. Black for Mef2A^H::Cre mice, D. Zhao, W. Yang, B. M. Steer, and M. Chalsev for technical support; the Gladstone Flow Cytometry and Histology Cores for technical support; and G. Howard for editorial assistance. *Irx3::EGFP* BAC transgenic mice were obtained from the Gene Expression Nervous System Atlas (GENSAT) Project (National Institute of Neurological Disorders and Stroke Contracts N01NS02331 and HHSN271200723701C to The Rockefeller University). S.-S.Z. was funded by the Heart and Stroke Foundation of Canada. S.-S.Z. and N.G. are funded by American Heart Association studentships and fellowships, respectively. J.W.S. was funded by the American Federation for Aging Research and by American Heart Association Grant SDG3420042. K.-H.K. and A.R. were supported by the Ontario Graduate Scholarship in Science and Technology and the Heart & Stroke Richard Lewar Centre of Excellence. A.R. was supported by a Heart and Stroke Foundation of Canada master's studentship. This work was funded by Canadian Institutes of Health Research grants (to C.-c.H. and P.H.B.); National Institutes of Health (NIH)/National Heart, Lung, and Blood Institute Grants R01 HL93414 ARRA (to B.G.B.) and R01 HL94414 (to R.M.S.); the Lawrence J. and Florence A. DeGeorge Charitable Trust/American Heart Association Established Investigator Award (to B.G.B.); NIH/National Center for Research Resources Grant C06 RR018928 (to the J. David Gladstone Institutes); and William H. Younger, Jr. (B.G.B.).

- Cohen SI, Lau SH, Stein E, Young MW, Damato AN (1968) Variations of aberrant ventricular conduction in man: Evidence of isolated and combined block within the specialized conduction system. An electrocardiographic and vectorcardiographic study. *Circulation* 38:899–916.
- Luliano S, Fisher SG, Karasik PE, Fletcher RD, Singh SN; Department of Veterans Affairs Survival Trial of Antiarrhythmic Therapy in Congestive Heart Failure (2002) QRS duration and mortality in patients with congestive heart failure. *Am Heart J* 143: 1085–1091.
- Rudy Y, Shaw RM (1997) Cardiac excitation: An interactive process of ion channels and gap junctions. *Adv Exp Med Biol* 430:269–279.
- Moskowitz IP, et al. (2007) A molecular pathway including *Id2*, *Tbx5*, and *Nkx2-5* required for cardiac conduction system development. *Cell* 129:1365–1376.
- Bakker ML, et al. (2008) Transcription factor *Tbx3* is required for the specification of the atrioventricular conduction system. *Circ Res* 102:1340–1349.
- Meysen S, et al. (2007) *Nkx2.5* cell-autonomous gene function is required for the postnatal formation of the peripheral ventricular conduction system. *Dev Biol* 303: 740–753.
- Rentschler S, et al. (2002) Neuregulin-1 promotes formation of the murine cardiac conduction system. *Proc Natl Acad Sci USA* 99:10464–10469.
- Hyer J, et al. (1999) Induction of Purkinje fiber differentiation by coronary arterialization. *Proc Natl Acad Sci USA* 96:13214–13218.
- Hall CE, et al. (2004) Hemodynamic-dependent patterning of endothelin converting enzyme 1 expression and differentiation of impulse-conducting Purkinje fibers in the embryonic heart. *Development* 131:581–592.
- Gómez-Skarmeta JL, Modolell J (2002) Iroquois genes: Genomic organization and function in vertebrate neural development. *Curr Opin Genet Dev* 12:403–408.
- Matsumoto K, et al. (2004) The prepattern transcription factor *Irx2*, a target of the FGF8/MAP kinase cascade, is involved in cerebellum formation. *Nat Neurosci* 7: 605–612.
- Bruneau BG, et al. (2001) Cardiomyopathy in *Irx4*-deficient mice is preceded by abnormal ventricular gene expression. *Mol Cell Biol* 21:1730–1736.
- Costantini DL, et al. (2005) The homeodomain transcription factor *Irx5* establishes the mouse cardiac ventricular repolarization gradient. *Cell* 123:347–358.
- Cohen DR, Cheng CW, Cheng SH, Hui CC (2000) Expression of two novel mouse Iroquois homeobox genes during neurogenesis. *Mech Dev* 91:317–321.
- Mummenhoff J, Houweling AC, Peters T, Christoffels VM, Rütger U (2001) Expression of *Irx6* during mouse morphogenesis. *Mech Dev* 103:193–195.
- Christoffels VM, Keijser AG, Houweling AC, Clout DE, Moorman AF (2000) Patterning the embryonic heart: identification of five mouse Iroquois homeobox genes in the developing heart. *Dev Biol* 224:263–274.
- Callahan CA, Thomas JB (1994) Tau-beta-galactosidase, an axon-targeted fusion protein. *Proc Natl Acad Sci USA* 91:5972–5976.
- Virágh S, Challice CE (1982) The development of the conduction system in the mouse embryo heart. *Dev Biol* 89:25–40.
- Miquerol L, et al. (2004) Architectural and functional asymmetry of the His-Purkinje system of the murine heart. *Cardiovasc Res* 63:77–86.
- Verzi MP, McCulley DJ, De Val S, Dodou E, Black BL (2005) The right ventricle, outflow tract, and ventricular septum comprise a restricted expression domain within the secondary/anterior heart field. *Dev Biol* 287:134–145.
- Danielian PS, Muccino D, Rowitch DH, Michael SK, McMahon AP (1998) Modification of gene activity in mouse embryos in utero by a tamoxifen-inducible form of Cre recombinase. *Curr Biol* 8:1323–1326.
- Delorme B, et al. (1997) Expression pattern of connexin gene products at the early developmental stages of the mouse cardiovascular system. *Circ Res* 81:423–437.
- Castellanos A, Jr., Maytin O, Arcebal AG, Lemberg L (1970) Significance of complete right bundle-branch block with right axis deviation in absence of right ventricular hypertrophy. *Br Heart J* 32:85–92.
- Nygren A, et al. (2000) Voltage-sensitive dye mapping of activation and conduction in adult mouse hearts. *Ann Biomed Eng* 28:958–967.
- Fast VG, Kléber AG (1995) Block of impulse propagation at an abrupt tissue expansion: evaluation of the critical strand diameter in 2- and 3-dimensional computer models. *Cardiovasc Res* 30:449–459.
- Fast VG, Kléber AG (1995) Cardiac tissue geometry as a determinant of unidirectional conduction block: Assessment of microscopic excitation spread by optical mapping in patterned cell cultures and in a computer model. *Cardiovasc Res* 29: 697–707.
- Myerburg RJ (1971) The gating mechanism in the distal atrioventricular conduction system. *Circulation* 43:955–960.
- Gourdie RG, et al. (1993) The spatial distribution and relative abundance of gap-junctional connexin40 and connexin43 correlate to functional properties of components of the cardiac atrioventricular conduction system. *J Cell Sci* 105:985–991.
- Bevilacqua LM, et al. (2000) A targeted disruption in connexin40 leads to distinct atrioventricular conduction defects. *J Interv Card Electrophysiol* 4:459–467.
- Kirchhoff S, et al. (1998) Reduced cardiac conduction velocity and predisposition to arrhythmias in connexin40-deficient mice. *Curr Biol* 8:299–302.
- Simon AM, Goodenough DA, Paul DL (1998) Mice lacking connexin40 have cardiac conduction abnormalities characteristic of atrioventricular block and bundle branch block. *Curr Biol* 8:295–298.
- Rackauska S, M, et al. (2007) Gating properties of heterotypic gap junction channels formed of connexins 40, 43, and 45. *Biophys J* 92:1952–1965.
- Lisewski U, et al. (2008) The tight junction protein CAR regulates cardiac conduction and cell-cell communication. *J Exp Med* 205:2369–2379.
- Cottrell GT, Burt JM (2001) Heterotypic gap junction channel formation between heteromeric and homomeric Cx40 and Cx43 connexons. *Am J Physiol Cell Physiol* 281: C1559–C1567.
- Cottrell GT, Burt JM (2005) Functional consequences of heterogeneous gap junction channel formation and its influence in health and disease. *Biochim Biophys Acta* 1711: 126–141.
- Valiunas V, Gemel J, Brink PR, Beyer EC (2001) Gap junction channels formed by coexpressed connexin40 and connexin43. *Am J Physiol Heart Circ Physiol* 281:H1675–H1689.
- Berger MF, et al. (2008) Variation in homeodomain DNA binding revealed by high-resolution analysis of sequence preferences. *Cell* 133:1266–1276.
- Noyes MB, et al. (2008) Analysis of homeodomain specificities allows the family-wide prediction of preferred recognition sites. *Cell* 133:1277–1289.
- Bilioni A, Craig G, Hill C, McNeill H (2005) Iroquois transcription factors recognize a unique motif to mediate transcriptional repression in vivo. *Proc Natl Acad Sci USA* 102:14671–14676.
- Chen ZQ, et al. (1995) Identification of two regulatory elements within the promoter region of the mouse connexin 43 gene. *J Biol Chem* 270:3863–3868.
- Chi NC, et al. (2008) Genetic and physiologic dissection of the vertebrate cardiac conduction system. *PLoS Biol* 6:e109.
- Kobayashi D, et al. (2002) Early subdivisions in the neural plate define distinct competence for inductive signals. *Development* 129:83–93.
- Chi NC, et al. (2010) Cardiac conduction is required to preserve cardiac chamber morphology. *Proc Natl Acad Sci USA* 107:14662–14667.
- Sharpe J, et al. (2002) Optical projection tomography as a tool for 3D microscopy and gene expression studies. *Science* 296:541–545.
- Zhou YQ, et al. (2004) Comprehensive transthoracic cardiac imaging in mice using ultrasound biomicroscopy with anatomical confirmation by magnetic resonance imaging. *Physiol Genomics* 18:232–244.